Article citation info:
SZYDLOWSKI, T., SICZEK, K., GLOGOWSKI, M. The effect of machined valve springs application on dynamic properties of electro-hydraulically driven valve train. *Combustion Engines*. 0000, **XXX**(X), xx-xx. https://doi.org/10.19206/CE-148172

Tomasz SZYDLOWSKI
Krzysztof SICZEK
Michal GLOGOWSKI

Combustion Engines
Polish Scientific Society of Combustion Engines

The effect of machined valve springs application on dynamic properties of electro-hydraulically driven valve train

ARTICLE INFO

Received: 1 February 2022
Revised: 31 March 2022
Accepted: 8 April 2022
Available online: 29 May 2022

Nowadays, the constant striving to reduce the emission and increase the overall efficiency over a wide range of speeds and loads of the internal combustion engine (CE) is observed. The different methods for improving the charge exchange in the engine, particularly ones based on the variable valve timing are sought. This variability can be achieved, among others by using the electrohydraulic valve drive. The goal of the present study is to compare the dynamic parameters of the engine valvetrain utilizing the unilateral electrohydraulic valve drive and various types of valve springs. The model of such a drive being developed by authors and experimentally verified was used for the analysis. Using the Finite Element Method, the models of springs made through the machining from single sleeves were developed. The effect of various geometrical parameters of the modernized springs on their stiffness and on the resulted valvetrain dynamics was examined.

Key words: *electro-hydraulic drive, valvetrain, machined valve spring, dynamics*

1. Introduction

Nowadays, many engines are equipped with camless valvetrain. One way to achieve camless valve operation is electrohydraulic valve control/actuation. Such valve drive converts fluid pressure into motion in response to a control signal. It could be realized as a one-side action drive or double-acting one. In the double-acting electrohydraulic drive (Fig. 1), the hydraulic oil causes the valve movement in both directions. The input for such a system is also current in the windings of the electromagnet. It generates the force exciting the movement of the distributor slider opening slits through which the operating fluid flows to and from the hydraulic cylinder. Upward movement of the slider (Fig. 2) causes the connection of space above the piston of the cylinder with a supply channel (of high pressure) and the simultaneous connection of space under the cylinder piston with return flow channel (of low pressure). The appearance of the different pressures on the sides of the piston leads to its movement – in this case, to open the valve. The return movement is also electrically excited. Changing the direction of current flow in the windings of the electromagnet leads to the generation of the force exciting movement of the distributor slider in the opposite direction. By moving down, the distributor slider first closes individual channels and then opens the connection between the supply channel and the space under the piston and the return channel and the space above the piston. The resulting pressure difference causes movement of the drive upwards. The movement ends with the closing of the valve. To prevent a situation in which the valve could remain unclosed, a spring holding the valve in the closed position can be used.

In this embodiment, the hydraulic oil causes movement of the valve in both directions. However, the valve is maintained in the upper position by a spring and not by the control system. This solution also eliminates the falling of the valves due to the pressure drop in the hydraulic system. This is important in the case of start-up when there is a possibility of valve collision with the bottom of the piston.

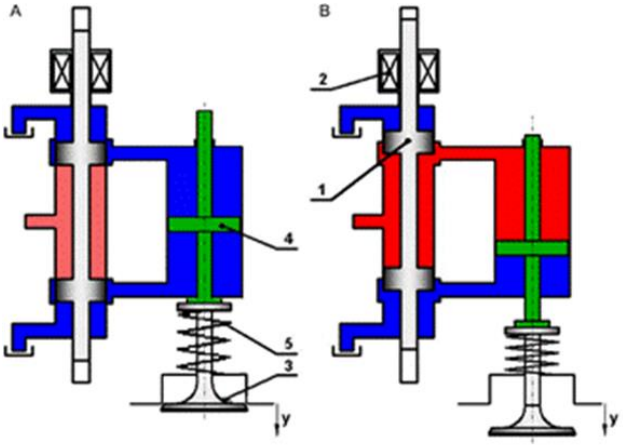

Fig. 1. Functional model of an electrohydraulic double-acting drive with spring outside the drive: 1 – slider of solenoid, 2 – electromagnetic coil; 3 – valve, 4 – cylinder piston, 5 – spring of cylinder piston (also valve spring)

Particularly, the spring position is outside the cylinder. The scheme of the drive valve system with the valve spring outside the cylinder is shown in Fig. 2. When the piston (Fig. 3, number 1) of the hydraulic drive (D) is in the upper position (UP) (Figure 2A) and operating oil pressure is not applied on its surface, the valve head (7) is pressed against its seat insert (8) by the valve spring (10). This pressure provides sealing of the valve.

With the start of oil flow at a predetermined pressure to the cylinder space, the piston (1) moves in the direction of the bottom position (BP) of the drive piston, causing compression of the spring (10) and opening the valve (V). This continues until the piston (1) meets the stop (5), limiting further movement of the piston (Fig. 2b). The piston moves in the section from UP to BP corresponding to piston stroke (S) equal to the stroke (H) of the valve (V). The drive operation is accompanied by the following impacts: one from the lower part of the piston (1) against the stop (5) and

another one from the head (7) of the valve (V) against its seat insert (8) at the time of closing of the valve. This requires the introduction of appropriate modifications to the schema of construction and operation of a one-side action hydraulic drive involving the use of braking of the so-called run piston before it reaches the extreme positions of the BP and UP.

Braking of this run piston is the reduction of the piston speed to zero at the end stages of its stroke. Selection of the piston braking performance, specifically the choice of suitable counter-braking characteristics, can only occur after the determination of the basic parameters of the hydraulic valve drive, which include the pressure of oil supplied to the hydraulic drive and courses of the piston movement corresponding to the courses of valve lift.

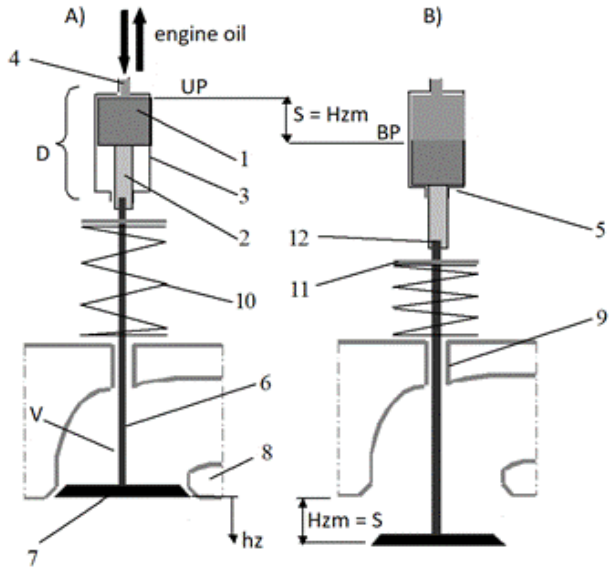

Fig. 2. Scheme of the electrohydraulic system: drive valve using a valve spring: (A) the drive (actuator) in a state corresponding to a closed valve, (B) the drive (actuator) in a state corresponding to an open valve; BP, bottom position of the drive piston; D, hydraulic drive (actuator); hz, valve lift; Hzm, valve stroke; S, stroke of drive piston; UP, the upper position of the drive piston, V – valve of engine: 1 – drive piston, 2 – piston rod, 3 – operating cylinder, 4 – inlet channel of operating (engine) oil, 5 – stop-limiting piston stroke, 6 – valve stem, 7 – valve head, 8 – seat insert, 9 – valve guide, 10 – valve spring, 11 – lock of the valve spring, 12 – connector between the valve and piston rod

There are many different realizations of electro hydraulically driven valvetrains applied both to combustion engines (CEs) and to the research stands used to investigation of variable valvetrains.

The correctness of operation of such systems is strongly affected by the features of engine oil used including degree of oxidation, degree of nitration, degree of sulfonation, water content, glycol content, total base number (TBN), total acid number (TAN) and kinematic viscosity at 40°C and 100°C, which varies during engine operation [21].

2. Realizations of electro hydraulically driven valvetrain

According to [19], many research groups have built at least a one-cylinder test engine for experimental tests, which increases the validity of the results.

The systems and studies of them are described in [1, 4-5, 10, 12-14, 16, 20, 22, 24-26, 34-38, 40-41, 47, 49**,** 50, 52, 55**,** 56, 61-64, 69, 76**,** 77, 79].

Commercially available research electrohydraulic variable valve actuation (VVA) systems are produced by Sturman Industries and Lotus Engineering [19]. Different mechanisms and solutions were developed and investigated in earlier research. Variable valve systems have often been designed to produce conventional or pure sinusoidal valve lift motion instead of optimized valve lift. In recent years, variable valve movement has been taken for granted, and research has concentrated on other areas, such as NO_x production, homogeneous charge compression ignition mixture control, and total controllability of the engine.

All VVA system publications have focused on small- and medium-bore engines (Ø120 mm bore), and gas exchange valve (GEV) strokes were mostly 6–10 mm (maximum, 12 mm), moving masses under 1 kg, and actuating forces a few hundred Newtons. Overall, no fully flexible valve actuation systems were found in the large-bore (Ø180 mm) engines, except in [1] and the two-stroke engine solutions of Wärtsilä and MAN B&W. All other large-bore-related systems were either "lost motion" or "hydraulic pushrod" types of systems in which the hydraulic pressure required by the GEV stroke is controlled by camshaft, which limits the operating range of the VVA system. On the other hand, two-stroke applications also have different requirements/boundary conditions due to moving masses, frequencies, and valve lifts. There is a lack of research on four-stroke large-bore systems.

Dresner and Barkan [16] provides a review and classification of variable valve timing mechanisms, in which 15 different VVA concepts are introduced. Large-bore two-stroke class engines have two commercial hydraulic actuated outlet valve systems: RT-Flex from Wärtsilä [8, 69, 74] and the MAN Diesel&Turbo (ME Intelligent engine) [68].

The sample realization of a double-acting system is the Ford concept given in [3]. It is the electrohydraulic system of variable control of timing, speed, and lift of the valves. The valves are opened and closed by hydraulic cylinders.

Another realization of the electrohydraulic system is the active double-action valve timing of Lotus (AVT) [54]. The system allows for individual control of valves and can perform a variety of valve lift profiles for different valves [39].

The system can open the valves more than once during the engine cycle [2, 54]. This system is used only for research purposes and is not suitable for mass-produced engines because the technology used is very expensive and fast servo valves do not allow control of the speed with sufficient accuracy at an engine speed greater than 4000 rpm [39]. Lotus and Eaton collaborated on the development of the AVT [72]. The AVT system was studied using a one-cylinder test engine [15].

In [27], the Jacobs VVT loss motion system called Evolve is presented. It can achieve degrees of early IVC, late IVC with partial lift, and early EVO. The system allows for a variable compression ratio to be obtained.

Sturman Industries elaborated the HVA system used in variable valve trains and in diesel injector technology [28, 71]. This system allows fine control of seating velocities

and the ability to respond to viscosity changes in working fluids. Sturman's hydraulic valve actuation system was implemented in several test engines from passenger cars to heavy duty trucks and some demonstration vehicles. Also, a module was developed for research purposes.

Fiat developed the electrohydraulic MULTIAIR system used in the Fiat Punto Evo [6]. In addition to eliminating the throttle valve, the intake side does not have a mechanical camshaft, but on the exhaust side generated pressure controlled by an electronic valve in each case works on one inlet valve. With the MULTIAIR system, five different operating modes are possible [29].

Reference [30] reported on the full variable valve train used in the BMW K71 tester engine. The valves are driven by a piezoelectric actuator with a hydraulic stroke ratio. Valve control with a piezoelectric actuator and hydraulic fluid allows for full dynamic variable inlet and outlet phasing, lift, opening time, and lift function.

Pournazeri [51] discussed a VVA system for a single engine valve studied on the tester. The system includes two rotary spool valves, two differential phase shifters, and a single-acting spring-return hydraulic cylinder for the engine valve connected to the piston of the cylinder.

Brader and Rocheleau [9] reported an electrohydraulic valve train in which the solenoid actuators were replaced with piezoelectric stacks. The proposed system is capable of a maximum valve lift of 12.4 mm and bandwidth frequency of up to 500 Hz.

Electrohydraulic valve drive systems can allow fully variable valve control. However, disadvantages of such systems are that they are expensive to manufacture due to the need for high precision and they require excessive energy consumption. In addition, there are changes in features of the operating medium, caused by changes in temperature.

One of electrohydraulic valve drive applied to the research stand was realized in the authors' department in the Lodz University of Technology. The numerical model of such a drive was also developed [65], experimentally verified [66] and used for simulation studies on different configurations of the chosen electrohydraulic valvetrain. The goal of the present study was to compare the dynamic parameters of the engine valvetrain utilizing the unilateral electrohydraulic valve drive and various types of both valve springs and valve materials. Ultimately, it is planned to create a subassembly of the test stand using the head of the internal CE with an electro-hydraulic valve drive and various configurations of valve springs.

Lou et al. [38] reported the electrohydraulic VVA system allowing continuously variable timing and two discrete lifts. The lift control was provided via a lift control sleeve hydraulically switching between two mechanically set positions to provide accurate lifts.

Nam et al. [41] presented the design and dynamic simulation of an electro-hydraulic camless engine valve actuator (EH-CEVA) and the experimental verification conducted using lift position sensors.

Giardiello et al. [20] proposed the utilizing of a 0D/1D CFD model of the entire electrohydraulic valvetrain VVA module, coupled with 1D lumped mass representing the inlet valve, for simulating of that valve motion and the interactions between flow and mechanical systems of the solenoid hydro-mechanical valve.

di Gaeta et al. [14] presented the mathematical model of an Electro-Hydraulic Valve Actuator (EHVA) prototype and the use of such a model for the design of cycle-by-cycle Valve Lift Control(VLC).

Zsiga et al. [79] reported the FlexWork valve train allowing the full variability for inlet and outlet valves and the cylinder deactivation.

Sun and Kuo [61] presented the transient control of a laboratory electro-hydraulic fully flexible valve actuation system. Such a control comprised transients of lift, duration, phase, speed, and mode of valves.

3. Valve springs in valvetrains of CEs

Vasilyev et al. [73] stated that the valve spring has the lowest stiffness and exhibits the lowest natural frequency compared to other valve train components.

Labore [32] noticed that there are several spring designs available today including the most popular cylindrical one, conical ones and beehive ones allowing reduction of movable masses and the use of the lighter retainers. The beehive ones can posses ovate wires providing a multi-arc design distributing more material into the high-stress portion of the spring, thus spreading out the stress load. Ovate wires also allow for higher lifts, require less space, thus allowing for their tighter packaging. The conical springs provide a much higher natural frequencies than the other designs.

Pal et al. [43] stated that in most of the cam valvetrains applied in the IC engines, valve helical compression springs are critical components absorbing energy while opening the valves and releasing energy at the closing of them. Spring stiffness plays a significant role in the design of each helical valve spring.

Materials and design of classical valve springs were discussed, inter alia, in [17].

Interestingly, Shiao et al. [58] proposed a variable valve actuation device of compact design and comprising a magnetorheological (MR) valve, passive buffer spring, cam, and rocker arm. They reported that the MR valve could effectively provide functions of variable valve timing and variable valve lift (VVL) via a dynamical control of the external current in the magnetic coil.

As stated in [67] a compression spring can control the motion by maintaining contact between two elements. Particularly, in a cam-follower arrangement, a spring provides contact between such elements parallelly controlling their motion.

Chime and Ukwuaba [11] reported five major metallurgical classifications of wire spring materials including high carbon steel, alloy steel, stainless steel, Ni-based alloys, and Cu-based alloys.

According to [67] various compression springs can be made from the following materials:

- Hard-drawn wire – applied for low stresses and static loads. It cannot be used at sub-zero temperatures and at temperatures above 120 deg C.
- High carbon blue tempered and polished spring steel – applicable for springs operating in a protected environment, as carbon steel can corrode without lubrication or sealing against the atmosphere influence.

- Oil tempered wire (cold drawn, quenched, and tempered) – not suitable for springs exposed to fatigue or sudden loads as well as at sub-zero temperatures and at temperatures above 180 deg C.
- Alloy steels with Cr and V – applied for high stress conditions and at high temperature up to 220 deg C. Springs made of these materials exhibit a good fatigue resistance and long endurance for shock and impact loads.
- Alloy steels with Cr and Al – applied for highly stressed springs requiring for long life and operating under shock loading and at temperatures up to 250^{o}C.
- Piano wire (made from tempered high carbon steel) – applied for small springs with a very high toughness and tensile strength, withstanding repeated loading at high stresses. They cannot be utilized at sub-zero temperature and the one above 120^{o}C.
- Stainless steel (with at least 10% Cr) – for springs with a high corrosion resistance, staining and corroding very slowly in severe environment like a seawater. Springs made of this material are applicable for temperatures up to 288^{o}C. These made from stainless steels of 18–8 composition can be utilized also for sub-zero temperatures.
- Phosphor bronze and brass – used as spring materials provide good corrosion resistance and electrical conductivity. They are normally used for contacts in electrical switches. Springs made of brass are applicable to sub-zero temperatures.

Wound wire springs are made of spring wire coiled hot or cold with ends configured within the limits of coil wire.

Boehm [7] reported that wire wound springs are usually made of medium and high strength steels, Ni alloys, Ti and stainless steels and undergone heat-treating and cold reduction. Machined springs use similar materials, however neither spring wire nor malleable bar can be applied for machined springs. A completed wound spring usually retains various amounts of residual stress despite the application of various stress relieving processes.

A machined spring with similar residual stress in the free state can exhibit unwanted free-state deformation. Low level of residual stress in such springs can be provided using martensitic corrosion resistant steels (CRES) and martensitic steels including moderate to high strength CRES, such as 17-4 PH per AMS5643, 15-5PH per AMS5659, CC455 per AMS5617, and very high strength steels like C300 per AMS6514.

The other appropriate group of materials for the machined springs comprises 7075-T6 Al (high strength), 7068-T6511 Al (very high strength), 38644 Beta C Ti (very high strength and corrosion resistant), Delrin 100 (machinable plastic), and Ultem 2300 (machinable plastic). The Al- and Ti-based cases are important from the point of view of the necessity to reducing movable masses in engine valvetrains.

Wound wire compression springs are often shot peened to increase the fatigue resistance. The gaps between the coils are usually wide enough to allow such a process related to the conditions allowing shot passing through and the surface exposure of coils.

Small coil slots of machined springs sometimes excluded possibility of shot passing through. In this case the fatigue resistance is providing by stress relief holes and slots added to the slot ends or by selection of high strength, fatigue-resistant materials.

Wire springs can be plated with Zn and Ni for corrosion protection. Plating machined springs is made harder by the sharp edge corners insufficient covered. Aluminum machined springs are typically anodized or coated to prevent corrosion.

Suda and Ibaraki [60] described trends in high strength steels for valve springs and development status of the super-high strength steels.

Boehm [7] noticed that although the machined springs function similarly to wire ones, they are manufactured starting usually from metal bar stocks. The latter are first machined into a thick wall tube form, from which a helical slot is cut revealing multiple coils. The final form when deflected, provides the desired elasticity.

The manufacturing of the machined springs is more expensive, involving more time and more specialized machines.

Valve spring usually posses round coils.

The machined compression springs can have square, or rectangular (radial or longitudinal) coils with an easily changeable sizes limited by no standard.

On wire wound compress springs, the space between the coils (slots) is uniform, with the end coils tending to taper to zero. These so called “closing” ends are obtainable in an additional forming process. Their optional grinding allows obtaining their nearly flatness.

Currently, machined springs can reach a minimum slot of about 0.51 mm. Wider slots, however, below 6.35 mm are also obtainable. The slot width can reach nearly zero value via a stress relieving process, but no pre-stressing is currently being met.

Machined springs has a limited number of coils up 30 coils depending on spring size, and commonly it is below 20.

Contrary to a wire spring, with the entire length of the wire contributing to the elasticity, for a machined one the flexure section providing the desired elasticity is captive between the end sections providing structure and attachment. The end sections possess infinite stiffness in comparison to the flexure. Additionally, the end slots do not taper to zero, but remain at the full or initial width visible under the free spring length conditions. Therefore, to reach the close elastic performance, machined springs should be longer than wire ones.

A dimension precision finer than 0.1% is not achievable available for wire wound springs but only for machined ones using post-processing techniques.

Because of the machining practicality the machining spring sizes are limited to the range 2.54–152 mm in diameter. The spring length can reach up to 610 mm, but this applies to the range 25.4–76 mm in diameter. For smaller or larger diameter springs should be shorter.

Compression springs are fully machined to make the ends flat and very perpendicular to the longitudinal axis of the spring.

While wire wound springs are limited to single start configurations, machined springs handle single and multiple starts allowing for a pure force reaction.

Multiple start springs allow for a pure force reaction. Hence, compression springs with multiple starts provide

elastic motion without the need of corrective torques compensating these from compression forces occurring at the spring coil's width center shifted from the spring centerline. In multiple start springs these torques resolve to zero within the body of the spring. In single start springs, wound or machined, such torques need be resolved at the interface between the spring and the components providing the force and deflection.

Up to five starts can be used to unify the lateral reaction of machined springs. Multiple starts also add to the length of machined springs. Should a failure occur, the remaining coil(s) provide some functionality albeit degraded due to the missing coil.

Stresses in both machined and wire wound compression springs are dominantly torsional shear. The maximum stresses are located on the spring inner diameter and on the coil sides. Such stresses occur very rare on the spring outer diameter. Stresses at the sharp corners are very low.

The stress relief holes (SRH) or elongated holes at the slot ends are beneficial for compressed machined springs.

Linearity of compression springs depends on:
- geometric changes in the spring during elastic deformation from free length,
- residual stresses in the material,
- enhancing coil contact during deflection,
- boundary condition fixation,
- spring rotation during deflection.

When helical springs are compressed, end-to-end twisting occurs. To eliminate the torsional deformation in machined springs the following remedies can be utilized:
- fixing the end of the spring via any of the attachment techniques,
- constraining the spring end to enhance the elastic rate,
- the use of two concentric springs one with a right-hand flexure and the other a left hand. The twisting of the inner spring counteracts that of the outer one.
- placing of two flexures on a single spring blank, one right hand and the other left hand. Such a configuration allows the interface between the two flexures to twist, while the ends are in rest.

Compression machined springs with multiple starts are predestined to the systems operating at resonance, due to their low tolerance elasticity, continuous slot dimension (no touching at coil ends at any time guarantees clean and quiet operation), internally resolved moments and uniform cross axis stiffness.

The compression springs may be prone to buckling, especially as the number of coils enhances.

Tsubouchi et al. [70] proposed a new and inexpensive forming method of coil springs with a rectangle cross-section with a high rectangular ratio. The coil springs, formed by the proposed method, with a cross-section of a high rectangular ratio possessed the lower spring constant, compared to those with a circular cross-section. Additionally, the work-hardening enlarged the elastic limit, and thus also the safety level of the formed coil springs, compared to the machined ones.

Nama [42] numerically studied the linear static and modal analysis of a helical machined spring. The conventional helical springs of different index with rectangular cross section area were compared with two machined helical springs, one with different slot hole diameter and the other with different end extension length.

For the machined helical spring it was found that the tangent-to-machining path hole configuration is better than the center-to-machining hole configuration and changing the extension length has no significant effect on spring characteristics. The machined spring with any slot hole and any extension length was better than the identical helical spring with rectangular cross section.

The important aspect of the design of valve springs is the method used for the modelling of the valve springs.

During simulations carried out by Prabakar and Mangalaramanan [48], the valve springs were modeled as flexible bodies. Each coil of the springs was modeled as a separate flexible body and contact between these coils was established.

To study the influence of the spring on the dynamic behavior of the whole valvetrain, Frendo [18] proposed a multi-mass spring model in which the mass points are connected by two series of elastic and damping elements, one for the elasto-dynamic characteristics and the other for the possibility of the spring coils to reach contact with each other.

Iritani et al. [31] reported a valve spring model utilizing a beam to couple the displacement and shearing stress with gap elements. In this manner, both the same-pitch valve spring and the different-pitch valve spring can be modeled. Hsu and Pisano [75], Lee and Patterson [33] utilized the wave equation to describe the displacement of the spring elements. Pisano [45, 46], Hanachi and Freudenstein [57], Paranjpe [44], Jang and Park [59], Rego and Martins [53] modelled the valve spring as a distributed parameter system.

Guo et al. [23] modelled the valve spring using the surge-mode approach in which the displacement of each spring element was governed by the wave equation.

Zheng et al. [78] developed a multi-body dynamic model of the valve mechanism based on the key performance and the structure parameters of the valve spring. Via the optimization strategy utilizing such a model, the oscillation amplitude of the valve spring was weakened by about 63%.

4. Methods and materials

The analysis is carried out using models of:
- the electro-hydraulic drive of valve,
- valve assembly,
- valve spring.

The valve assembly contained valve, valve cap and valve stem locks. The geometry parameters were the same for all cases considered. The mass of valve cap and valve stem locks were also unchanged. The mass of valve depended on valve design and material. The classical valve spring geometry was the same for all cases considered. Its mass and characteristics depend on the material.

4.1. Model of electrohydraulic valve drive

Figure 3 shows diagram of the hydraulic drive with valve and valve spring. This drive is the single-acting drive. It consists of hydraulic distributor and hydraulic actuator. Between the engine valve 5 and the piston 3 there is the valve spring 4, which is responsible for closing the valve and maintains it in the closed position, providing a leak-

proof of the valve seat. Current in the electromagnet coil is the control signal forcing the movement of the valve. The engine oil is the working medium, which causes displacement of the piston to the bottom, and thus moves the engine valve. This oil flows into the space above the piston through oil channel O_2, from supply channel O_1 after turning on the current in the coil of the electromagnet 2 – Fig. 3b. Then slide of the distributor is moved to the right side and opens the gap, through which the oil flows from the supply channel O_1 to channel O_2. When changing the direction of current flow in the windings of the electromagnet, slider 1 moves to the left to its initial position, causing closure of the supply channel O_1 and the opening of the return channel O_3. The oil now flows from the oil space above piston 3, causing suddenly reduction of the pressure. This reduction of the oil pressure above the piston of the cylinder in combination with the force of the valve spring 4 moves the piston up and closes the engine valve 5 (Fig. 3a).

Prior to testing, the following assumptions were made:

– opening of the valve will last as short as possible,
– final phase of valve closing aim to slow down the valve speed, so that eventually it will shut down with as low speed as possible but without a significant extension of the whole closing phase,
– drive control will be limited to step signal.

This means that the controller can only change the duration of the bipolar signal depending on the angular velocity of the engine crankshaft.

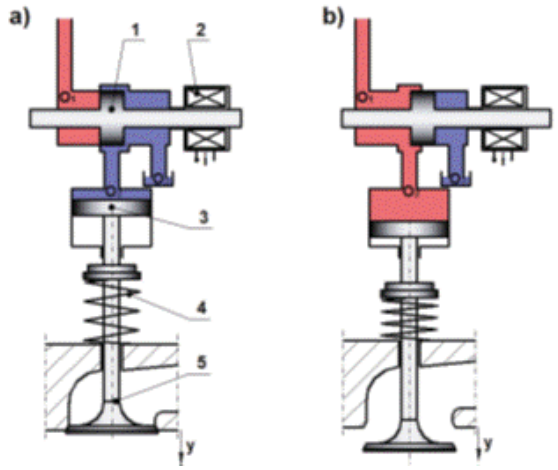

Fig. 3. The diagram of single-acting hydraulic drive: 1 – slider of electrovalve, 2 – electromagnet coil, 3 – piston of the actuator, 4 – actuator piston spring (valve spring), 5 – valve, O1, O2, O3 – oil channels

Considering the control of the electrohydraulic drive one must consider several important issues. First, start of movement of the valve is significantly delayed in opposition to the control signal, which results from the experimental research [9]. This delay time consists of:

time between start of control signal and beginning of the movement of the servo valve spool (1–2 ms) and the rise time of the corresponding actuator pressure, needed to move off the engine valve (1.5–3 ms). For this reason, the control of this valve drive cannot be done in real time, after start of the control signal at the time corresponding to one position of the crankshaft.

Therefore, to obtain the relevant moments of opening and closing of the valve (crankshaft angles), the control system should obtain a signal, for the time no less than equal to the delay time, before reaching the engine crankshaft position corresponding to the opening of the valve. This will be possible only, if the control system will solicit engine operation parameters in the form of feedback. These parameters, necessary for control signals, will include mainly the angular velocity of the engine crankshaft and the temperature of the working medium. If the control system will be the adaptive system, the angles of rotation of the crankshaft, which took place at the opening and closing of the valve and the actual valve lift must be taken into consideration, too.

Sample waveform of the valve lift is shown in Fig. 4. To obtain such a waveform, control signal with the following components is required:

1. the duration of the valve opening signal – t_o,
2. the duration of the valve closing signal – t_z,
3. the duration of the valve braking signal – t_h.

During valve lift the delay time of the drive was labeled as t_{zz}.

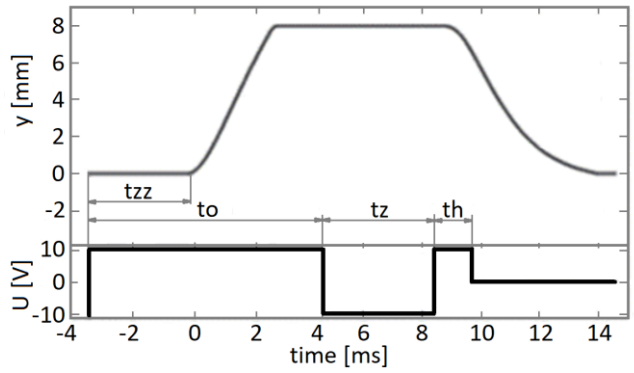

Fig. 4. Characteristic parameters of the control signal necessary to achieve the desired waveform of the valve lift

The duration of valve opening signal will depend mainly on the angular speed of the engine crankshaft. The duration of the closing signal and the braking signal will be fixed for specific ranges of supply pressures and speeds of the crankshaft, which will be achieved with the full opening of the valve, as demonstrated below.

Previous studies (mainly experimental) have shown that minimum valve closing speed for supply pressure 10 MPa was approximately 0.26 m/s. Such speed, from the viewpoint of valve subsidence in the seat, seems acceptable. Valve closing time for such speed, however, would be about 30 ms.

Full opening of the return gap allowed to reach for the valve closing speed is up to 3 m/s. Valve closing time for such speed would be about 3 ms. The aim of the simulation was, inter alia, propose such a method of controlling, to give as small as possible valve closing speed and not significantly increase valve closing time.

4.2. Model of electrohydraulic valve drive using the Rexroth servo valve

The concept and operating phases of the single-acting hydraulic drive with the Rexroth servo valve are shown in

Fig. 5. The basic element of the drive is the single-acting hydraulic cylinder 1, which opens the valve of the internal CE 2. The return spring 3 closes the valve. The operation of the drive is controlled by a distributor 4 (which connects the actuator either to the power supply or to the tank).

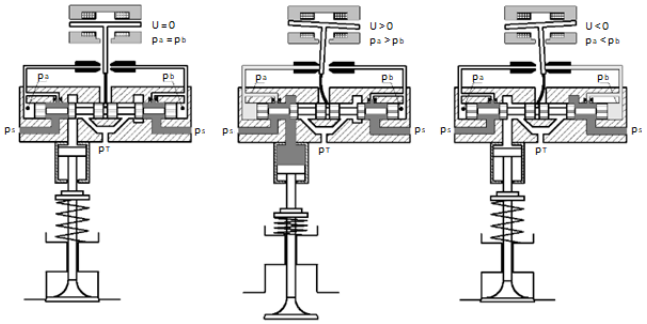

Fig. 5. Operating phases of electrohydraulic valve drive with the Rextrox servo valve

4.2.1. Mathematical model of the drive

Considering the complex structure of the model electro-hydraulic valve drive when developing its mathematical model, the whole system was divided into fragments (sub-models). For further considerations, the following model structure was adopted using the following markings:
SM – torque control motor model,
WH – hydraulic amplifier model,
SS – servo spool model,
RH – hydraulic distributor model,
SH – hydraulic cylinder model.

Initial condition related to the rest of all movable components. The boundary conditions were determined by the existing geometrical limits resulted from the design of the drive. Within such limits the related displacements were allowed between movable and immovable components, assumed to be rigid bodies.

4.2.1.1. Torque control actuator model

The servo control actuator converts the current signal to the proportional angular movement of the armature. The armature, made of magnetic material, is mounted elastically with a thin-walled tube in which the diaphragm is routed. The moment acting on the armature is proportional to the control current.

Considering the system of forces acting on the armature of the torque actuator according to Fig. 6, considering its small angular displacements, the equation of armature rotational motion relative to its axis of rotation assumes:

$$J_z \frac{d^2\varphi}{dt^2} = M_z - k_z \cdot \varphi - c_z \frac{d\phi}{dt} - F_h \cdot l_h - F_s \cdot l_s \qquad (1)$$

where: J_z – mass moment of inertia of the armature relative to its axis of rotation, φ – armature rotation angle, k_z – tube stiffness, c_z – armor viscosity resistance coefficient, M_z – armature torque, where: F_h – hydrodynamic force acting on the nozzle diaphragm, where: l_h – distance between the armature rotation axis and the nozzle axis,
$F_s = k_s \cdot (x + \varphi \cdot l_s)$ – spring force, where: k_s – spring elasticity coefficient, l_s – distance between the armature rotation axis and the end of the spring.

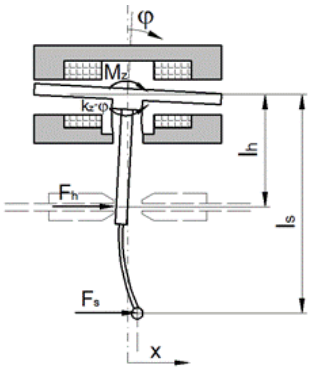

Fig. 6. Diagram of the torque control engine

The drive input control signal will be the voltage signal. Therefore, to assume small angular displacement of the armature, the relationship between the input voltage signal applied to the torque motor coils and the current can be described by the following equation:

$$L \cdot \frac{di}{dt} = U - R \cdot i \qquad (2)$$

where: L – inductance of coils, R – coil resistance, U – voltage.

4.2.1.2. Model of a hydraulic amplifier

Torque motor armature is rigidly connected to the nozzle diaphragm, which in functional terms belongs to a hydraulic amplifier. This is a nozzle-aperture amplifier. The angular movement of the armature causes the nozzle aperture to deflect and change its distance from the nozzles. This leads to a decrease in pressure before the exposure nozzle and an increase in pressure before the exposure nozzle – Fig. 7. The resulting pressure difference is used to change the position of the servo valve control spool.

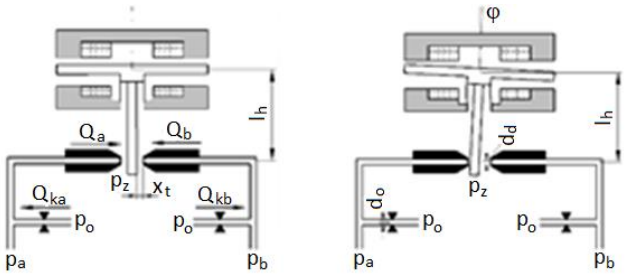

Fig. 7. Diagram of the electrohydraulic amplifier

The pressure connected to the supply system is p_0. These channels are separated by flanges with diameters d_0 connecting them with working channels a and b, in which pressures p_a and p_b prevail.

Therefore, the flow rate through the individual nozzles of the hydraulic amplifier is:

$$Q_{k_a} = Q_a + Q_{h_w} + Q_{cw} \qquad (3)$$

$$Q_{k_b} = Q_b - Q_{h_w} + Q_{cw} \qquad (4)$$

where: $Q_{ka} = c_q \cdot \frac{\pi \cdot d_0^2}{4} \cdot \sqrt{\frac{2 \cdot (p_0 - p_a)}{\rho}}$ – flow rate through the orifice 'a', where: c_q – flow factor, d_0 – diameter of the

orifice, $Q_{kb} = c_q \cdot \frac{\pi \cdot d_0^2}{4} \cdot \sqrt{\frac{2 \cdot (p_0 - p_b)}{\rho}}$ – flow rate through orifice "b", $Q_a = c_q \cdot \pi \cdot d_d \cdot (x_t - \phi \cdot l_h) \cdot \sqrt{\frac{2 \cdot (p_a - p_z)}{\rho}}$ – flow rate through the nozzle 'a', where: d_d – nozzle diameter, x_t – distance between the aperture and the nozzle in the middle position of the armature, $Q_b = c_q \cdot \pi \cdot d_d \cdot (x_t + \phi \cdot l_h) \cdot \sqrt{\frac{2 \cdot (p_b - p_z)}{\rho}}$ – flow rate through the nozzle 'b', $Q_{hw} = A_s \frac{dx}{dt}$ – slider absorbency, where: $A_s = \frac{\pi \cdot d_s}{4}$ – slider face area, where: d_s – diameter of the four-edge slider, x – slider shift, $Q_c = \frac{V_k}{E_c} \cdot \frac{dp_{a/b}}{dt}$ – flow rate covering losses due to compressibility of the liquid, where: E_c – modulus of elasticity of liquids, V_k – chamber volume.

4.2.1.3. Servo valve slider model

The equation of motion of the four-edge slider has the form:

$$m_s \cdot \frac{d_s^2 x}{dt^2} = \Delta p_s \cdot A_s - F_s - F_{hd} - F_t \cdot \mathrm{sgn}\left(\frac{dx}{dt}\right) - c_s \cdot \frac{dx}{dt} \quad (5)$$

where: m_s – mass of the four-edge slider, x – slider shift, Δp – differential pressure of front faces of the piston (nozzle inlets), $F_{hd} = \frac{0{,}72}{\sqrt{\xi}} \cdot \pi \cdot d_s \cdot x \cdot \Delta p_s = k_{hd} \cdot x \cdot \Delta p_s$ – hydrodynamic force acting on the slider, where: ξ – coefficient of flow resistance through the gap, Δp_s – pressure drop across the slider gap, F_t – static friction force, c_s – coefficient of viscosity of the slider.

4.2.1.4. Hydraulic distributor model

The movement of the four-edge slider opens and closes the gap connecting the cylinder chamber with the supply and drainage channel.

For the analyzed solution, the value of the flow rate through the working gap can be described by the relationship derived from the Bernoulli equation:

$$Q = c_q \cdot \sqrt{\frac{2}{\rho}} \cdot \pi \cdot d_s \cdot x_r \cdot \sqrt{\Delta p} = K_Q \cdot x_r \cdot \sqrt{\Delta p} \quad (6)$$

where: c_q – flow factor depending on Reynolds number, x_r – gap opening depends on the displacement of the four-edge slider, $K_Q = c_q \cdot \sqrt{\frac{2}{\rho}} \cdot \pi \cdot d_s$ – flow factor depending on the geometry of the gap, Reynolds number and density of the working medium, p – pressure drops across the gap.

The equation of flow through the servo valve takes the form:

$$Q_S = Q_T + Q_h + Q_p + Q_c \quad (7)$$

where: $Q_S = K_{QS} \cdot x_{rS} \cdot \sqrt{p_S - p_A}$ – supply flow rate, $Q_T = K_{QT} \cdot x_{rT} \cdot \sqrt{p_A - p_T}$ – drainage flow rate, where: p_S – supply pressure, p_A – pressure in the working chamber, p_T – pressure in the drainage channel, $Q_p = k_v \cdot p_A$ – leakage flow rate, where: k_v – leakage factor, $Q_h = A \frac{dy_p}{dt}$ – the absorber capacity of the actuator, where: A – working surface of the actuator piston, y_p – displacement of the gym piston rod $Q_c = \frac{V_0 + A \cdot y_p}{E_c} \cdot \frac{dp_A}{dt}$ – flow rate covering losses due to compressibility of the liquid, where: E_c – bulk modulus of liquids, V_0 – volume of the chamber.

4.2.1.5. Hydraulic distributor model

The equation of actuator valve movement can be presented in the following form:

$$\begin{cases} m \cdot \frac{d^2 y}{dt^2} + C \cdot \frac{dy}{dt} + F_t \cdot \mathrm{sign}\left(\frac{dy}{dt}\right) + k \cdot y \\ = A \cdot p_A + m \cdot g - k \cdot y_0 - F_g \text{ for } y < y_{pmax} \\ \\ m_v \cdot \frac{d^2 y}{dt^2} + C_v \cdot \frac{dy}{dt} + F_{tv} \cdot \mathrm{sign}\left(\frac{dy}{dt}\right) + k \cdot y \\ = m \cdot g - k \cdot y_0 - F_g \text{ for } y > y_{pmax} \end{cases} \quad (8)$$

where: m – sum of masses: piston with piston rod, engine valve and elements connected to it, m_v – mass of engine valve and components connected to it, y – motor valve displacement, y_0 – preload of the valve spring, C, C_v – coefficients of viscous friction, respectively for combined actuator and valve and the valve itself, F_t, F_{tv} – static friction forces, k – valve spring coefficient of elasticity, A – cylinder piston surface area, p_A – pressure in the actuator, $F_g = A_z \cdot p_s(t)$ – gas force acting on the valve head, where: A_z– surface area of the valve head, $p_s(t)$ – gas pressure in the engine cylinder.

4.3. Parameters of valve and classical valve spring

During analysis were used two valves: the full one made of steel (chosen as the reference one) and the full one made of Ti-Al alloy. The electro-hydraulically driven valve cooperated with a classical valve spring made of steel. Its parameters were presented in Table 1. Alternatively, valve can mate with the machined spring.

Table 1. Specifications of the analyzed vehicle

Parameter	Designation	Values
Steel valve mass	m_v [g]	41
TiAl valve mass		27
Valve stem lock mass	m_{vsl} [g]	1
Valve cap mass	m_{vc} [g]	6
Spring mass	m_s [g]	22
Valve seat diameter	D_{vs} [mm]	27.7
Valve stroke	H [mm]	8
Spring wire diameter	d [mm]	2.8
Inner diameter of spring	D_i [mm]	14.1
Outer diameter of spring	D_{out} [mm]	19.7
Initial length of spring	L_0 [mm]	46.9
Pre-tension displacement of spring	L_1 [mm]	12
Force relative to pre-tension displacement of spring	F_1 [N]	210
Maximum displacement of spring	L_2 [mm]	20
Force relative to maximal displacement of spring	F_2 [N]	370

4.4. The model of the machined spring

The model of machined spring was elaborated using the FEM. Geometry of such a model was presented in Fig. 8A. The grid of tetragonal elements was shown in Fig. 8B. The boundary conditions were following:

– bottom plane of spring was fixed,
– the top plane of spring was loaded by the force with a set value from the range 0–370 N.

During analysis, it was assumed, that reference machined spring rate was the same as for the classical steel valve spring. Also, its loads were assumed to be the same. The machined spring was obtained from single sleeve by removing material in the form of the coil with constant rectangular cross-section. The pitch of that coil was equal to 5 mm and number of its wings was equal to 8. It was assumed that Yield stress for the spring steel was equal to 1300 MPa.

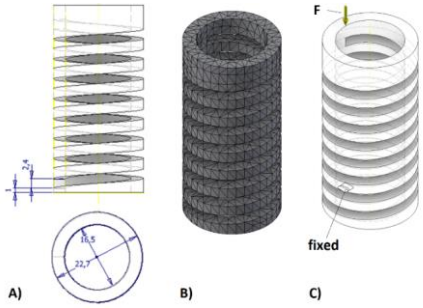

Fig. 8. Model of machined spring. A) geometry, B) grids of the finite elements, C) coundary conditions

5. Results

The obtained mass of the reference machined spring was equal to 39 g which was 72% higher than the mass of classical steel spring.

The obtained values of von-Misses stresses in of the steel machined spring with the removed coil pitch equal to 5 mm are presented in Fig. 9. The maximal value was higher only by 1.8% from the assumed Yield stress.

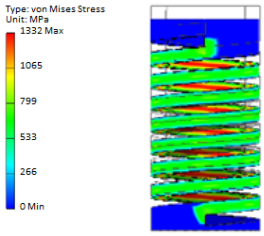

Fig. 9. von Misses stresses in the steel machined spring with the removed coil pitch equal to 5 mm

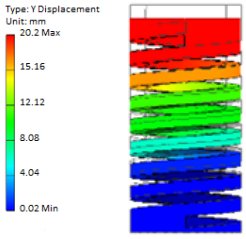

Fig. 10. Axial displacements of machined spring with the removed coil pitch equal to 5 mm

The obtained axial displacements for of the steel machined spring with the removed coil pitch equal to 5 mm were presented in Fig. 10. The maximal value differed by 1% from those of the classical steel spring.

The obtained values of von-Misses stresses in the steel machined spring with the removed coil pitch equal to 5.1 mm were presented in Fig. 11. The maximal value was lower by 3% from the assumed Yield stress.

The obtained axial displacements for of the steel machined spring with the removed coil pitch equal to 5.1 mm were presented in Fig. 12. The maximal value differed by 7% from those of the classical steel spring.

The obtained values of von-Misses stresses in the steel machined spring with the removed coil pitch equal to 4.9 mm were presented in Fig. 13. The maximal value was higher by 9% from the assumed Yield stress.

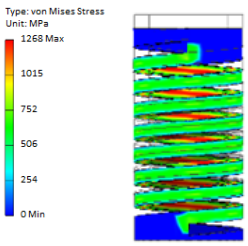

Fig. 11. von-Misses stresses in the steel machined spring von-Misses stresses in the steel machined spring with the removed coil pitch equal to 5.1 mm

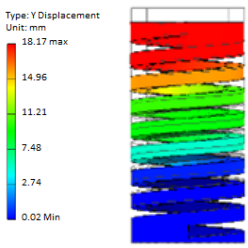

Fig. 12. Axial displacements of machined spring with the removed coil pitch equal to 5.1 mm

The obtained axial displacements for of the steel machined spring with the removed coil pitch equal to 4.9 mm were presented in Fig. 14. The maximal value differed by 10% from those of the classical steel spring.

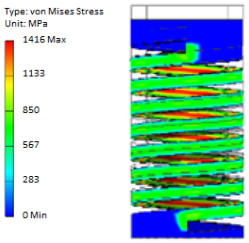

Fig. 13. von-Misses stresses in the steel machined spring von-Misses stresses in the steel machined spring with the removed coil pitch equal to 4.9 mm

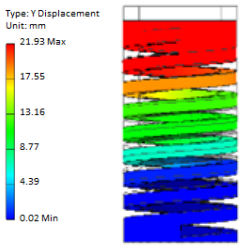

Fig. 14. Axial displacements of machined spring with the removed coil pitch equal to 4.9 mm

The obtained values of von-Misses stresses in the steel machined spring with the removed coil pitch equal to 5 mm and mean diameter increased by 1 mm were presented in Fig. 15. The maximal value was higher by 18% from the assumed Yield stress.

The obtained axial displacements for of the steel machined spring with the removed coil pitch equal to 5 mm and the mean diameter increased by 1 mm were presented in Fig. 16. The maximal value differed by 3% from those of the classical steel spring.

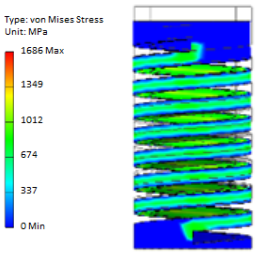

Fig. 15. von-Misses stresses in the steel machined spring von-Misses stresses in the steel machined spring with the removed coil pitch equal to 5 mm and mean diameter increased by 1 mm

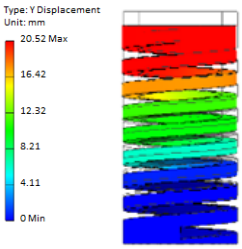

Fig. 16. Axial displacements of machined spring with the removed coil pitch equal to 5 mm and the mean diameter increased by 1 mm

The obtained values of von-Misses stresses in the steel machined spring with the removed coil pitch equal to 5 mm and mean diameter decreased by 1 mm were presented in Fig. 17. The maximal value was higher only by 1% from the assumed Yield stress.

The obtained axial displacements for of the steel machined spring with the removed coil pitch equal to 5 mm and the mean diameter decreased by 1 mm were presented in Fig. 18. The maximal value differed by 0.5% from those of the classical steel spring.

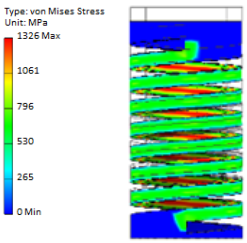

Fig. 17. von-Misses stresses in the steel machined spring von-Misses stresses in the steel machined spring with the removed coil pitch equal to 5 mm and mean d diameter increased by 1 mm

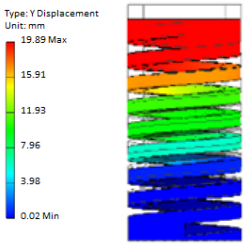

Fig. 18. Axial displacements of machined spring with the removed coil pitch equal to 5 mm and the mean diameter decreased by 1 mm

The obtained courses of valve lift versus time for analyzed vales and spring configurations were shown in Fig. 19. It was visible, that for the TiAl valve obtained maximal valve lifts were slightly higher than in case of the valve made of steel. Also, when using classic valve spring the valve lifts were slightly higher than in case of machined spring. The rising of valve was quicker when mating with the classic spring compared to the case of the machined spring. The falling of TiAl valve was quicker in the case of TiAl valve compared to the steel valve. The use of machined spring resulted in slightly longer falling period of TiAl valve, but in slightly shorter falling period of the steel valve compared to the case of classic valve spring.

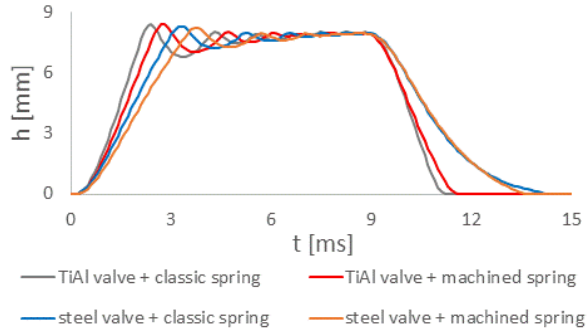

Fig. 19. The courses of engine valve lift versus time for the steel valve mating with the classic valve spring, the steel valve mating with the machined valve spring, the TiAL valve mating with the classic valve spring and the TiAl valve mating with the machined valve spring

For the 4-stroke engine speed equal to 3000 rpm, from the obtained courses of valve lifts versus time the relating values of valve angle-cross-sections were estimated. Calculations of the latter were carried out related to the camshaft rotates. The resulting values were presented in Table 2. Interestingly, the angle-cross-section obtained for the steel valve mating with machined valve spring was lower by 2.6% than that obtained in case of classical spring. The angle cross-sections for valve made of TiAl alloy were lower by 5.6% and 5.5% when mating with classical spring and machined one, respectively, compared to the case of steel valve mating with classical spring.

Table 2. The angle-cross-sections for valve driven electrohydraulically

Valve material	Type of valve spring	Angle-cross-section [deg·mm]
Ti-Al alloy	Classical	554.96
	Machined	554.41
Steel	Classical	587.45
	Machined	571.99

The obtained courses of related valve acceleration versus time for analyzed valves and spring configurations were shown in Fig. 20. It was seen that near the theoretical extreme positions of valve the damped vibration or/and impacts occurred. The amplitude of vibrations near the maximal valve lift was higher for the case of TiAl valve up to 3% compared to the case of the steel one. The highest amplitude of vibration occurred for the valve made of TiAl alloy mating with the classic valve spring. The smallest amplitude occurred for steel valve mating with the machined spring. The impact resulted in high amplitude of acceleration occurred during valve settling was much stronger for the valve made of TiAl alloy compared to the steel one. For the case of valve made of TiAl alloy the impact was stronger by up to 30% when it mated with classic spring compared to the case of the machined one. For the case of steel valve, the mentioned impact was stronger up to 50% in case of mating with the machined spring than in case of the classical spring.

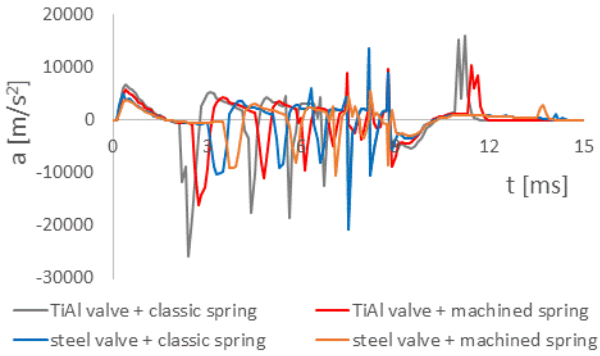

Fig. 20. The courses of engine valve acceleration versus time for the steel valve mating with the classic valve spring, the steel valve mating with the machined valve spring, the TiAl valve mating with the classic valve spring and the TiAl valve mating with the machined valve spring

The mentioned results of valve lifts and acceleration depended primarily on the total mass of valve and mating valve spring and by the relatively simple control scheme of medium pressure in the modelled drive. The geometry and material parameters of components in the modelled drive assembly and environmental parameters were not changed when analyzing individual configurations.

The simple control system used in the model of the currently existing research stand can be used to simulation

tests of classic steel valves and machined springs. But it turned out to be not very effective for light valves made of TiAl alloy and classic springs. Therefore, it will be necessary to introduce changes in CE involving the use of stronger vibration dampers, and earlier additional braking of the valve. You will probably need to introduce a more effective negative feedback control valve based on tracking its current position and acceleration and their deviations from the allowable values.

6. Summary

Under the same characteristic of the machined spring as the classic valve spring, the mass of the machined spring is greater. The use of machined spring made longer valve rising period but differently influenced the valve falling period depending on the valve mass. The use of the lightweight valve made shorter both valve rising and falling periods. It also resulted in higher amplitude of vibrations occurring near maximal valve lift and much stronger impact during valve settling compared to the heavier steel valve. To obtain the smoother courses of the valve lifts versus time from the model of the existing research stand it is necessary to add stronger vibration dampers, and earlier braking of the valve before its close position.

Nomenclature

BP	bottom position	MR	magnetorheological
CE	combustion engine	SI	spark ignition
CFD	computational fluid dynamics	SRH	stress relief holes
EH-CEVA	electro-hydraulic camless engine valve actuator	UP	upper position
GEV	gas exchange valve	VVA	variable valve actuation
IC	internal combustion	VVL	variable valve lift

Bibliography

[1] AALTONEN, J., VILENIUS, M. Control and controllability of electrohydraulic valvetrain in high and medium speed diesels. *SAE Technical Paper* 2002-01-2175. 2002. https://doi.org/10.4271/2002-01-2175

[2] ALLEN, J., LAW, D. Advanced combustion using a Lotus active valve train. Internal exhaust gas recirculation promoted auto ignition. *IFP International Congress* 2001.

[3] ALLEN, J., LAW, D. Production electro-hydraulic variable valve-train for a new generation of I.C. engines. *SAE Technical Paper* 2002-01-1109. 2002. https://doi.org/10.4271/2002-01-1109

[4] ANDERSON, M., TSAO, T., LEVIN, M. Adaptive lift control for a camless electrohydraulic valvetrain. *SAE Technical Paper* 981029. 1998. https://doi.org/10.4271/981029

[5] BATTISTONI, M., MARIANI, F., FOSCHINI, L. A parametric optimization study of a hydraulic valve actuation system. *SAE Technical Paper* 2008-01-1356. 2008. https://doi.org/10.4271/2008-01-1356

[6] BERNARD, L., FERRARI, A., MICELLI, D. et al. Elektrohydraulische Ventilsteuerung mit dem "MultiAir" –Verfahren. *Motortechnische Zeitschrift.* 2009, **70**(12), 892-899.

[7] BOEHM, G.L. Wire Springs or Machined Springs? Design World, May 13, 2007. https://www.designworldonline.com/wire-springs-or-machined-springs/ (accessed on February 01, 2022).

[8] BOLETIS, E., KYRTATOS, A., YILDIRIM, T. et al. A new fuel injection and exhaust valve actuation system for a two-stroke engine family in the 30 to 50 cm bore segment. *CIMAC Congress* 2010. Paper No. 101, Bergen 2010.

[9] BRADER, J.S., ROCHELEAU, D.N. Development of a piezo electrically-controlled hydraulic actuator for a camless engine. Part 1. *Proceedings of the Institution of Mechanical Engineers, Part D: Journal of Automobile Engineering.* 2004, **218**(8), 817-822. https://doi.org/10.1243/0954407041581084

[10] CHEN, J. Electro-hydraulic fully flexible valve actuation system for engine test cell. *SAE Technical Paper* 2010-01-1200. 2010. https://doi.org/10.4271/2010-01-1200

[11] CHIME, R.O., UKWUABA, S.I. Design, modeling, simulation and analysis of compression spring. *International Journal of Engineering Science and Innovative Technology* (*IJESIT*). 2016, **5**(1), 1-13.

[12] DENGER, D., MISCHKER, K. The electro-hydraulic valvetrain system EHVS – system and potential. *SAE Technical Paper* 2005-01-0774. 2005. https://doi.org/10.4271/2005-01-0774

[13] DE OJEDA, W., FERNANDEZ, J. Hydraulic needle valve actuator and its application to a camless engine. *ASME, IMECE* 2003-43607. 2003, 39-44. https://doi.org/10.1115/IMECE2003-43607

[14] DI GAETA, A., VELASCO, C.I.H., GIGLIO, V. Modelling of an electro-hydraulic variable valve actuator for camless engines aimed at controlling valve lift parameters. *International Journal of Control*. 2021, **94**(10), 2857-2873. https://doi.org/10.1080/00207179.2020.1737333

[15] DITTRICH, P., PETER, F., HUBER, G. et al. Thermodynamic potentials of a fully variable valve actuation system for passenger-car diesel engines. *SAE Technical Paper* 2010-01-1199. 2010. https://doi.org/10.4271/2010-01-1199

[16] DRESNER, T., BARKAN, P. A review and classification of variable valve timing mechanisms. *SAE Technical Paper* 890674. 1989. https://doi.org/10.4271/890674

[17] EDWARDS, G.D. Valve-spring materials and design. *Industrial Lubrication and Tribology*. 1983, **35**(2), 44-51. https://doi.org/10.1108/eb053262

[18] FRENDO, F., VITALE, E., CARMIGNANI, L. et al. Development of a Lumped–parameter model for the dynamic analysis of valve train systems. *SAE Technical Paper* 2004-32-0051. 2004. https://doi.org/10.4271/2004-32-0051

[19] HERRANEN, M. Fully variable valve actuation in large bore diesel engines. *PhD Thesis*. Tampere University of Technology, Tampere 2014.

[20] GIARDIELLO, G., GIMELLI, A., DE NOLA, F. Engine valvetrain lift prediction using a physic-based model for the electronic control unit calibration. *E3S Web of Conferences*. 2020, **197**, 06015. https://doi.org/10.1051/e3sconf/202019706015

[21] GOLEBIOWSKI, W., WOLAK, A., ZAJAC, G. Definition of oil change intervals based on the analysis of selected

physicochemical properties of used engine oils. *Combustion Engines*. 2018, **172**(1), 44-50. https://doi.org/10.19206/CE-2018-105

[22] GU, Y., LI, H., LIU, F. et al. Study on modeling of electro-hydraulic variable valve mechanism based on CATIA. *International Conference on Future Power and Energy Engineering ICFPEE 2010*; June 26-27, 2010, Chenzen, China, 2010.

[23] GUO, J., ZHANG, W., ZOU, D. Investigation of dynamic characteristics of a valve train system. *Mechanism and Machine Theory*. 2011, **46**(12), 1950-1969. https://doi.org/10.1016/j.mechmachtheory.2011.07.014

[24] HERRANEN, M., HUHTALA, K., VILENIUS, M. et al. The electro-hydraulic valve actuation (EHVA) for medium speed diesel engines – development steps with simulations and measurements. *SAE Technical Paper* 2007-01-1289. 2007. https://doi.org/10.4271/2007-01-1289

[25] HERRANEN, M., VIRVALO, T., HUHTALA, K. et al. Comparison of control strategies of an electro-hydraulic valve actuation system. *SAE Technical Paper* 2009-01-0230. 2009. https://doi.org/10.4271/2009-01-0230

[26] HERRANEN, M., VIRVALO, T., HUHTALA, K. et al. Valve train with learning control features. *CIMAC Congress* 2010. Paper No. 68, Bergen 2010.

[27] http://www.jacobsvehiclesystems.com/files/media/Product/Evolve_production.pdf (accessed on February 01, 2022).

[28] http://sturmanindustries.com/Solutions/Products/HVACamless/HydraulicValveActuation/tabid/202/Default.aspx (accessed on February 01, 2022).

[29] http://www.schaeffler.com/remotemedien/media/_shared_media/08_media_library/01_publications/schaeffler_2/symposia_1/downloads_11/schaeffler_kolloquium_2010_18_en.pdf. (accessed on February 01, 2022).

[30] http://ic.daad.de/johannesburg/document/2013/extra2/NMMU3%20Becker%20Full%20variable%20valve%20train%20on%20a%20combustion%20engine.pdf (accessed on February 01, 2022).

[31] IRITANI, T., SHOZAKI, A., SHENG, B. et al. Prediction of the dynamic characteristics in valve train design of a diesel engine. *SAE Technical Paper* 2002-32-1839. 2002.

[32] LABORE, E. Valve spring tech: overview of valve spring design, dynamics. Chevy Hardcore, May 17, 2016. https://www.chevyhardcore.com/tech-stories/engine/valve-spring-tech-overview-of-valve-spring-design-dynamics/ (accessed on February 01, 2022).

[33] LEE, J., PATTERSON, D.J. Nonlinear valve train dynamics simulation with a distributed parameter model of valve springs. *ASME Journal of Engineering for Gas Turbines and Power*. 1997, **119**(3), 692-698. https://doi.org/10.1115/1.2817043

[34] LIU, J.R., JIN, B., XIE, Y.J. et al. Research on the electro-hydraulic variable valve actuation system based on a three-way proportional reducing valve. *International Journal of Automotive Technology*. 2009, **10**(1), 27-36.

[35] LIU, F., LI, H., GAO, F. et al. A new electro-hydraulic variable valve-train system for IC engine. *IEEE 2nd International Asia Conference on Informatics in Control, Automation and Robotics* (CAR) 6-7 March 2010, Wuhan 2010, 174-179.

[36] LOU, Z. Camless variable valve actuation designs with two-spring pendulum and electrohydraulic latching. *SAE Technical Paper* 2007-01-1295. 2007. https://doi.org/10.4271/2007-01-1295

[37] LOU, Z., DENG, Q., WEN, S. et al. Progress in camless variable valve actuation with two-spring pendulum and electrohydraulic latching. *SAE International Journal of Engines*. 2013, **6**(1), 319-326. https://doi.org/10.4271/2013-01-0590

[38] LOU, Z., WEN, S., QIAN, J. et al. Camless variable valve actuator with two discrete lifts. *SAE Technical Paper* 2015-01-0324. 2015. https://doi.org/10.4271/2015-01-0324

[39] MILOVANOVIC, N., TURNER, J., KENCHINGTON, S. et al. Active valvetrain for homogenous charge compression ignition. *International Journal of Engine Research*. 2005, **6**(4), 377-397. https://doi.org/10.1243/146808705X30396

[40] MURATA, Y., KUSAKA, J., ODAKA, M. et al. Achievement of medium engine speed and load premixed diesel combustion with variable valve timing. *SAE Technical Paper* 2006-01-0203, 2006. https://doi.org/10.4271/2006-01-0203

[41] NAM, K., CHO, K., PARK, S. et al. Design and performance evaluation of an electro-hydraulic camless engine valveactuator for future vehicle applications. *Sensors*. 2017, **17**, 2940. https://doi.org/10.3390/s17122940

[42] NAMA, S.A. Modeling and Analysis of a Helical Machined Springs. *The Iraqi Journal for Mechanical and Material Engineering*. 2015, **15**(2), 152-163.

[43] PAL, S., SINGH, S.K., BHARTI, S.K. et al. Design and analysis of engine valve spring. *International Journal of Scientific & Engineering Research*. 2020, **11**(6), 337-340.

[44] PARANJPE, R.S. Dynamic analysis of a valve spring with a Coulomb-friction damper. *ASME Journal of Mechanical Design*. 1990, **112**(4), 509-513. https://doi.org/10.1115/1.2912639

[45] PISANO, A.P. FREUDENSTEIN. F. An experimental and analytical investigation of the dynamic response of a high-speed cam-follower system. Part 1: experimental investigation. *ASME Journal of Mechanisms, Transmissions, and Automation in Design*. 1983, **105**(12), 692-698. https://doi.org/10.1115/1.3258538

[46] PISANO, A.P., FREUDENSTEIN, F. An experimental and analytical investigation of the dynamic response of a high-speed cam-follower system. Part 2: a combined, lumped/distributed parameter dynamic model. *ASME Journal of Mechanisms, Transmissions, and Automation in Design*. 1983, **105**(12), 699-704. https://doi.org/10.1115/1.3258539

[47] PLÖCKINGER, A. Comparison of three different concepts for a variable valvetrain for huge combustion engines. *Proceedings of the 3rd FPNI PhD symposium*. Terrassa 2004, 453-462.

[48] PRABAKAR, R., MANGALARAMANAN, S. Flexible multi-body dynamic analysis of multi-cylinder engine valve train. *SAE Technical Paper* 2011-26-0086. 2011. https://doi.org/10.4271/2011-26-0086

[49] POSTRIOTI, L., BATTISTONI, M., FOSCHINI, L. et al. Application of a fully flexible electrohydraulic camless system to a research SI engine. *SAE Technical Paper* 2009-24-0076, 2009. https://doi.org/10.4271/2009-24-0076

[50] POSTRIOTI, L., FOSCHINI, L., BATTISTONI, M. Experimental and numerical study of an electro-hydraulic camless VVA system. *SAE Technical Paper* 2008-01-1355, 2008. https://doi.org/10.4271/2008-01-1355

[51] POURNAZERI, M. Development of a new fully flexible hydraulic variable valve actuation system. *PhD Thesis*. University of Waterloo, Waterloo, Ontario 2012.

[52] RICHMAN, R., REYNOLDS, W. A computer-controlled poppet-valve actuation system for application on research engines. *SAE Technical Paper* 840340. 1984. https://doi.org/10.4271/840340

[53] REGO, R.A., MARTINS, J.G. Valve motion modelation for use in airflow engine simulation. *SAE Technical Paper* 2001-01-3958. 2001. https://doi.org/10.4271/2001-01-3958

[54] SCHECHTER, M., LEVIN, M. Camless engine. *SAE Technical Paper* 960581. 1996. https://doi.org/10.4271/960581

[55] SCHEIDL, R., WINKLER, B. Model relations between conceptual and detail design. *Mechatronics.* 2010, **20**, 842-849.
[56] SCHNEIDER, W. Fully variable, simple, and efficient electrohydraulic valve train for reciprocating engines. *12th International Fluid Power Conference*. Dresden 2020. **3**(3), 181-189. https://doi.org/10.25368/2020.107
[57] HANACHI, S, FREUDENSTEIN. F. The development of a predictive model for the optimization of high-speed cam-follower systems with Coulomb damping internal friction and elastic and fluidic elements. *Journal of Mechanisms Transmissions and Automation in Design*. 1986, **108**(12), 506-515. https://doi.org/10.1115/1.3258762
[58] SHIAO, Y., KANTIPUDI, M.B., JIANG, J.W. Novel spring-buffered variable valve train for an engine using magneto-rheological fluid technology. *Frontiers in Materials*. 2019, **6**, 95. https://doi.org/10.3389/fmats.2019.00095
[59] JANG, S., PARK, K. Dynamic EHL film thickness in cam and follower contacts of various valve lifts. *SAE Technical Paper* 2000-01-1789. 2000. https://doi.org/10.4271/2000-01-1789
[60] SUDA, S., IBARAKI, N. The past and future of high-strength steel for valve springs. *KOBELCO Technology Review*. 2005, **26**, 21-25.
[61] SUN, Z., KUO, T. Transient control of electro-hydraulic fully flexible engine valve actuation system. *IEEE Transactions on Control Systems Technology*. 2010, **18**(3), 613-621. https://doi.org/10.1109/TCST.2009.2025188
[62] SUN, Z. Electrohydraulic fully flexible valve actuation system with internal feedback. *Journal of Dynamic Systems, Measurement, and Control*. 2009, **131**(2), 024502. https://doi.org/10.1115/1.3072146
[63] SUN, Z., HE, X. Development and control of electro-hydraulic fully flexible valve actuation system for diesel combustion research. *SAE Technical Paper* 2007-01-4021. 2007. https://doi.org/10.4271/2007-01-4021
[64] SUN, Z., CLEARY, D. Dynamics and control of an electro-hydraulic fully flexible valve actuation system. *IEEE Proceedings of the American Control Conference*. 2003, **4**, 3119-3124.
[65] SZYDLOWSKI, T., SMOCZYNSKI, M. Model of hydraulic single acting drive for valves of internal combustion engines. *Journal of KONES Powertrain and Transport*. 2009, **16**(1), 465-472.
[66] SZYDLOWSKI, T. Experimental verification of the model of electrohydraulic drive for internal combustion engine valves. *Journal of KONES Powertrain and Transport*. 2009, **16**(3), 401-408.
[67] TABUÑARFORTUNADO, I., FORTUNADO, I. The spring as a simple machine. *IOSR Journal of Applied Physics.* 2019, **11**, 57-61. https://doi.org/10.9790/4861-1102025761
[68] The intelligent engine: Development status and prospects. http://www.mandieselturbo.com/files/news/filesof769/Int%20Eng%20Prospects.pdf (accessed on February 01, 2022).
[69] The Sulzer RT-flex common-rail system described. ftp://vk.od.ua/20011.pdf (accessed on February 01, 2022).
[70] TSUBOUCHI, T., TAKAHASHI, K., KUBOKI, T. Development of coiled springs with high rectangular ratio in cross-section. *Procedia Engineering*. 2014, **81**, 574-579. https://doi.org/10.1016/j.proeng.2014.10.04
[71] TURNER, C., BABBITT, G., BALTON, C. et al. Design and control of a two-stage electrohydraulic valve actuation system. *SAE Technical Paper* 2004-01-1265. 2004. https://doi.org/10.4271/2004-01-1265
[72] TURNER, J., KENCHINGTON, S., STRETCH, D. Production AVT development: Lotus and Eaton's electrohydraulic closed-loop fully variable valve train system. *25th International Vienna Motor Symposium*. Vienna 2004.
[73] VASILYEV, A.V., BAKHRACHEV, Y.S., STOROJAKOV, S.Y. Dynamics simulation model for the internal combustion engine valve gear. *Procedia Engineering*. 2016, **150**, 312-317. https://doi.org/10.1016/j.proeng.2016.07.017
[74] Wärtsilä RT-flex 50 technology review. http://engine.od.ua/ufiles/Wartsila-20041.pdf (accessed on February 01, 2022).
[75] HSU, W.S. PISANO, A.P. Modeling of a finger-follower cam system with verification in contact forces. *ASME Journal of Mechanical Design*. 1996, **118**(5), 132-137. https://doi.org/10.1115/1.2826844
[76] WU, H., CHEN, J., LI, M. et al. Iterative learning control for a fully flexible valve actuation in a test cell. *SAE Technical Paper* 2012-01-0162. 2012. https://doi.org/10.4271/2012-01-0162
[77] XIE, Y. GAO, Z., JIN, B. et al. Frequency response enhancement of variable valve system by employing peak and hold method. *Indian Journal of Engineering and Materials Sciences*. 2010, **17**(4), 275-281.
[78] ZHENG, H., YAN, F., LU, C. et al. Optimization design of the valve spring for abnormal noise control in a single-cylinder gasoline engine. *Proceedings of the Institution of Mechanical Engineers, Part D: Journal of Automobile Engineering.* 2017, **231**(2), 204-213. https://doi.org/10.1177/0954407016651180
[79] ZSIGA, N., OMANOVIC, A., SOLTIC, P. et al. Functionality and potential of a new electrohydraulic valve train. *MTZ Worldwide.* 2019, **80**, 18-27. https://doi.org/10.1007/s38313-019-0086-0

Tomasz Szydlowski, DEng. – Department of Vehicles and Fundamentals of Machine Design, Lodz University of Technology, Poland.
e-mail: *tomasz.szydlowski@p.lodz.pl*

Michał Głogowski, DEng. – Faculty of Process and Environmental Engineering, Lodz University of Technology, Poland
e-mail: *michal.glogowski@p.lodz.pl*

Krzysztof Siczek, DSc., DEng. – Department of Vehicles and Fundamentals of Machine Design, Lodz University of Technology, Poland.
e-mail: *ks670907@p.lodz.pl*